

# Scanning Electron Microscopy

---

Volume 1985 | Number 3

Article 2

---

8-7-1985

## Fundamental Aspects of Energetic Particle/Solid Interactions

Nicholas Winograd

*The Pennsylvania State University*

Follow this and additional works at: <https://digitalcommons.usu.edu/electron>



Part of the [Biology Commons](#)

---

### Recommended Citation

Winograd, Nicholas (1985) "Fundamental Aspects of Energetic Particle/Solid Interactions," *Scanning Electron Microscopy*. Vol. 1985 : No. 3 , Article 2.

Available at: <https://digitalcommons.usu.edu/electron/vol1985/iss3/2>

This Article is brought to you for free and open access by the Western Dairy Center at DigitalCommons@USU. It has been accepted for inclusion in Scanning Electron Microscopy by an authorized administrator of DigitalCommons@USU. For more information, please contact [digitalcommons@usu.edu](mailto:digitalcommons@usu.edu).



FUNDAMENTAL ASPECTS OF ENERGETIC PARTICLE/SOLID INTERACTIONS

Nicholas Winograd

Department of Chemistry  
The Pennsylvania State University  
152 Davey Laboratory  
University Park, PA 16802  
Phone No. (814) 863-0001

(Paper received February 28, 1985: manuscript received August 07, 1985)

Abstract

The interaction of keV particles with solids has been characterized by the measurement of the angle and energy distribution of sputtered secondary ions and neutrals. The results are compared to classical dynamics calculations of the ion impact event. Examples using secondary ions are given for clean Ni(001), Cu(001) reacted with O<sub>2</sub>, Ni(001) and Ni(7 9 11) reacted with CO, and Ag(111) reacted with benzene. The neutral Rh atoms desorbed from Rh(001) are characterized by multiphoton resonance ionization of these atoms after they have left the surface.

Introduction

The collision of a keV heavy particle with a solid initiates a complex series of events which ultimately leads to the ejection of a variety of atomic and molecular species. The composition of these species are often characteristic of the original make-up of the target. Whether dealing with a low dose Secondary Ion Mass Spectrometry (SIMS) experiment or a focussed primary beam used for ion microscopy, it is necessary to obtain a detailed understanding of the ion bombardment event to appreciate the mechanisms involved in the ejection process. In a global sense, there are two phenomena which need to be examined. The first is to predict the nuclear motion in the solid which gives rise to the ejection of atoms and the second is to evaluate the inelastic events that give rise to excited species and secondary ions. The first aspect of the problem has been extensively developed utilizing a straightforward classical dynamics model to follow the flow of energy through the lattice for the first picosecond or so after bombardment.<sup>(15)</sup> The ionization problem is much more difficult, although progress is now being made using a number of approaches.

It is our view that in order to compare experimental measurements to the emerging theoretical predictions, it is necessary to be very careful in specifying the type of sample to be studied and in defining the measurement conditions as precisely as possible. In this paper, we report on a series of experiments aimed at measuring the yield of secondary ions and neutrals as a function of their take-off angle and their kinetic energy. This approach, rather than measuring angle and energy-integrated yields, allows much more detailed comparisons to theory and makes the testing of proposed models much more straightforward.

Key words: Ion Beams, Surfaces, Ion Bombardment, Laser Ionization Sputtering, Sputtering Theory, Adsorption, Particle/Solid Interactions, Secondary Ion Mass Spectrometry

Angular Distributions of Secondary Ions from Clean Single Crystal Surfaces

Using the general experimental and theoretical approach described above, it is now our goal to see what type of structure-

sensitive information exists in the angular distributions of the secondary ions. As Wehner showed many years ago, the distributions of the neutrals are highly anisotropic and very clearly reflect the surface symmetry. There have been many attempts to explain these distributions. One such explanation is that the ejection occurs along close-packed lattice directions which extend deep within the crystal.<sup>(13)</sup> This idea nicely explained the peaks in the angular distributions but required that there be quite a bit of long range order in the solid even during the impact event. That requirement seems a bit hard to swallow in view of the extensive damage that is created within the crystal. Although controversy existed concerning these "focusons" for many years, the molecular dynamics calculations of Harrison clearly showed that the ejection was dominated by near surface collisions rather than those from beneath the surface.<sup>(6)</sup>

The results of calculations are displayed schematically in Figure 1, where a {001} crystal

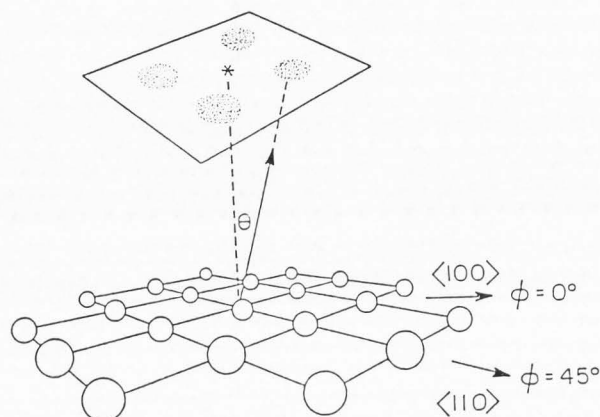


Figure 1. Coordinate system used in determining angular distributions.

face is given as an example. Here, each atom's ultimate fate is plotted as a point on a plate high above the solid. Atoms that are ejected perpendicular to the surface ( $\theta = 0^\circ$ ) are plotted in the center of the plate.

The molecular dynamics calculations yield a clear picture of the scattering mechanisms that give rise to these angular anisotropies, particularly for the higher kinetic energy atoms. Most of the ejected particles arise from within two or three lattice spacings from the impact point and suffer only a few scattering events. The spacings between the surface atoms exert a strong directional effect during ejection. Note that most particles are ejected along  $\phi = 0^\circ$ , since there are no atoms in the surface to block their path. The nearest neighbor atom along  $\phi = 45^\circ$  inhibits ejection in this direction. It is possible, using the apparatus shown in Figure 2, to compare the measured angular distributions of secondary ions to the calculated distributions for a clean

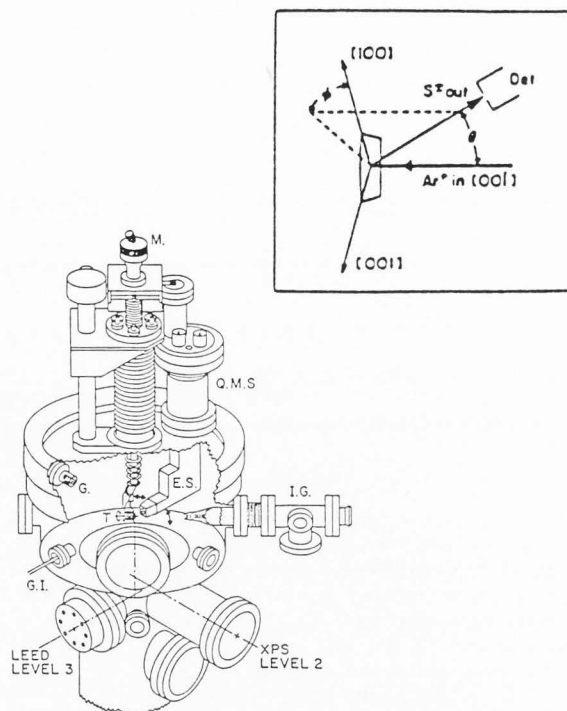


Figure 2. Schematic view of the spectrometer. The components illustrated include M, crystal manipulator; Q.M.S., quadrupole mass spectrometer; I.G., primary ion source; E.S., energy spectrometer; G, Bayard-Alpert gauge; T, crystal target; and G.I., gas inlet. Auxiliary components are omitted for graphical clarity. The SIMS experimental geometry and coordinate system are defined in the inset. From reference 7.

Ni{001} single crystal surface.<sup>(7)</sup> The results of this comparison are shown in Figure 3.<sup>(6)</sup> Each panel represents an azimuthal angle scan at a particular polar angle. The calculated curves have been corrected for the presence of an image force which tends to bend the secondary ions toward the surface plane. The agreement between the two curves is reasonable under all conditions. Note that in accord with the schematic presentation in Figure 1, the secondary ion intensity maximizes at  $\phi = 0^\circ$  and minimizes at  $\phi = 45^\circ$  for  $\theta \geq 45^\circ$ . Thus it appears that in this simple situation, ion angular distributions behave similarly to the neutrals and are well-predicted by theory.

#### Angular Distributions of Secondary Ions from Adsorbate Covered Surfaces

The channeling phenomena observed from clean surfaces should also be found in more complex systems such as metals covered with a chemisorbed layer. For these cases, there are various ways in which one might envision the

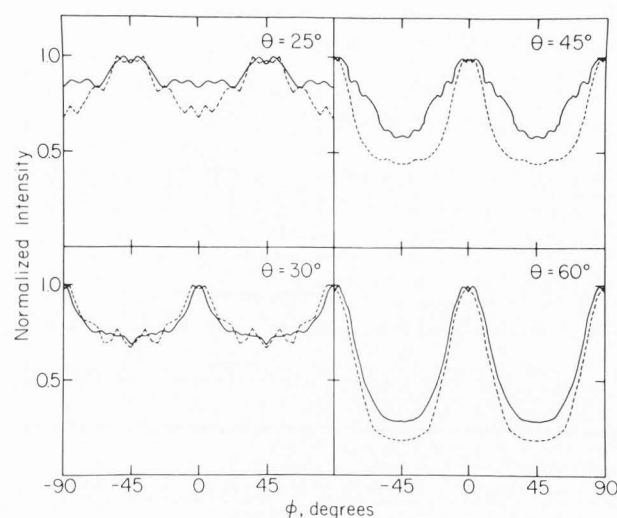


Figure 3. Dependence of  $\text{Ni}^+$  ion yield on azimuthal angle at various polar angle for clean  $\text{Ni}(001)$  bombarded by 1500 eV  $\text{Ar}^+$  ions at normal incidence. The solid curves represent experimental data while the dashed curves are predicted values obtained by correcting the calculated yields for 1000 eV  $\text{Ar}^+$  ion bombardment for the presence of the image force. Only those particles with a kinetic energy of  $4 \pm 4$  eV were detected. From reference 6.

angle to be important. Examples of azimuthal anisotropies have already been seen for the case of clean metals where surface channeling and blocking give rise to the observed effect. This situation should also apply to adsorbate covered surfaces. Other possibilities include the study of anisotropies in the polar angle distributions as well as in the yield of particles due to changes in the angle of incidence of the primary ion.

Considerable progress in quantitatively describing the ejection of chemisorbed atoms and molecules from metals has been made using molecular dynamics calculations. The main difficulty in describing any situation like this is to develop appropriate interaction potentials which describe the scattering events. Since little is known about these potentials, early calculations have utilized pair-wise additive potentials for adsorbates which have the same form as for the substrate, but with different mass. The exact form of the potential is not as critical as the atomic placement of the adsorbate atom. Thus, in the calculation, the geometry and coverage of the adsorbate may be varied over a wide range to test how these quantities influence ejection mechanisms and ultimately the angular distributions. In this section, examples of how several different experimental configurations can be utilized will be reviewed.

### Atomic Adsorbates

The first application of angle-resolved SIMS to the determination of the surface structure of chemisorbed layers is for oxygen adsorbed on the  $\{001\}$  face of  $\text{Cu}$ .<sup>(9)</sup> In this situation, the oxygen overlayer forms a  $c(2 \times 2)$  structure as determined by low energy electron diffraction (LEED). Classical dynamics calculations indicate that the oxygen should be ejected in the  $\phi = 0^\circ$  direction if it is originally bonded above the copper atom, because it is directly in the path of the ejected substrate species. However, if the oxygen is in a hole site, bonded to four substrate atoms, its predicted angle of ejection is  $\phi = 45^\circ$ . Experimental studies have confirmed that the oxygen resides in a fourfold bridge site because it is ejected in the  $\phi = 45^\circ$  direction.<sup>(9)</sup>

There is a number of complications associated with this simple interpretation. First, the magnitude of the azimuthal anisotropies are dependent upon the kinetic energy of the desorbing ion. For the very low energy particles, there has been sufficient damage to the crystal structure near the impact point of the primary ion that the channeling mechanisms are no longer operative. On the other hand, at higher kinetic energies, say greater than 10 eV, the desorbing ion leaves the surface early in the collision cascade while there is still considerable order in the crystal. The channeling mechanisms are much stronger and the angular anisotropies are larger.

A second complication involves the determination of the height of the adsorbate atom above the surface plane. Calculations have been performed where this bond distance has been varied over several Angstroms in order to find the best fit with experiment.<sup>(9,11)</sup> These studies have also shown that there is a sensitivity of the polar angle distribution to the effective size of the adsorbed atom. Thus, it is important to know more about the scattering potential parameters if this distance is to be determined accurately. It appears, however, that the type of adsorption site may be determined in a reasonably straightforward manner.

### Adsorption of CO on $\text{Ni}\{001\}$

The response of a surface, to ion bombardment, covered with a molecularly adsorbed species is mechanistically distinct from the atomic adsorbate case. For CO on  $\text{Ni}\{001\}$ , for example, the strong C-O bond of 11.1 eV and the weak Ni-CO bond of 1.3 eV allow the CO molecule to leave the surface without fragmentation. In the experimental studies, the main peaks in the SIMS spectra for a  $\text{Ni}\{001\}$  surface exposed to a saturation coverage of CO are  $\text{Ni}^+$ ,  $\text{Ni}_2^+$ ,  $\text{Ni}_3^+$ ,  $\text{NiCO}^+$ ,  $\text{Ni}_2\text{CO}^+$ , and  $\text{Ni}_3\text{CO}^+$ . All ions show a smooth increase in intensity with CO adsorption and reach saturation after 2-L CO exposure (0.5 monolayer coverage). The yields of  $\text{C}^+$ ,  $\text{O}^+$ ,  $\text{NiC}^+$  and  $\text{NiO}^+$ , are all less than 0.01 of the  $\text{Ni}^+$  intensity.

The classical dynamics treatment for CO on  $\text{Ni}\{001\}$  yields results which are in qualitative agreement with these findings. Approximately 80%

of the CO molecules that eject are found to eject intact, without rearrangement. The formation of  $\text{NiCO}$  and  $\text{Ni}_2\text{CO}$  clusters have been observed over the surface via reactions of Ni atoms and CO molecules. No evidence has been found for  $\text{NiC}$  and  $\text{NiO}$  clusters in the calculations. The ion bombardment approach, then, is a very sensitive probe for distinguishing between molecular and dissociative adsorption processes.

A number of workers have attempted to identify structural relationships found using other techniques such as LEED and vibrational spectroscopy to cluster yields in SIMS. The correlation of  $\text{Ni}_2\text{CO}^+$  to bridge-bonded CO and  $\text{NiCO}^+$  to linear bonded CO is an example of this approach. As it happens, the calculations clearly show that the mechanism of cluster formation is not consistent with this picture since the clusters form over the surface via atomic collisions. Furthermore, combined LEED/SIMS results indicate that the cluster ion yields are not directly related to the adsorbate/substrate geometry.<sup>(10)</sup> The  $c(2 \times 2)$  structure of CO on  $\text{Ni}(001)$  with all the molecules in the A-top site gave the same  $\text{Ni}_2\text{CO}^+/\text{NiCO}^+$  ratio as the compressed hexagonal LEED structure which must have both A-top and bridge-bonded CO molecules.

On the other hand, it is clear that angular distributions for atomic adsorbates are very sensitive to the surface structure so it is not unreasonable to anticipate similar effects for the Ni/CO system. Extensive calculations using the molecular dynamics procedure<sup>(6)</sup> have been completed for the A-top and twofold bridge bonding configurations but statistical considerations have restricted the analysis to only the Ni atoms. As shown in Figure 4 when the CO is in the A-top geometry, the calculated Ni distributions peak along azimuthal directions which are similar to the clean surface. For the twofold bridge case, however, the CO overlayer tends to randomly scatter the ejecting Ni atoms producing a much different pattern.<sup>(16)</sup> The predictions for the A-top bonding geometry, when corrected for the presence of the image force, are in quite good agreement with experiment, and are consistent with the wide range of other experimental data available for the system.

#### Adsorption of CO on $\text{Ni}(7 \times 9 \times 11)$

Since the azimuthal angle distributions are sensitive to subtle differences between surface structures, it is of interest to examine the role of larger surface irregularities such as surface steps on the measured quantities. For example, suppose the orientation of the primary ion beam in the SIMS experiment is fixed at different azimuthal angles with respect to the step edge. If the ejection process is structure-sensitive, then changes in yield and cluster formation probabilities should be observed as the ion bombards "up" or "down" the steps. In addition, the desorption of chemisorbed molecules should be influenced by their proximity to the step edge.

Carbon monoxide chemisorption on  $\text{Ni}(7 \times 9 \times 11)$  represents an interesting case with which to

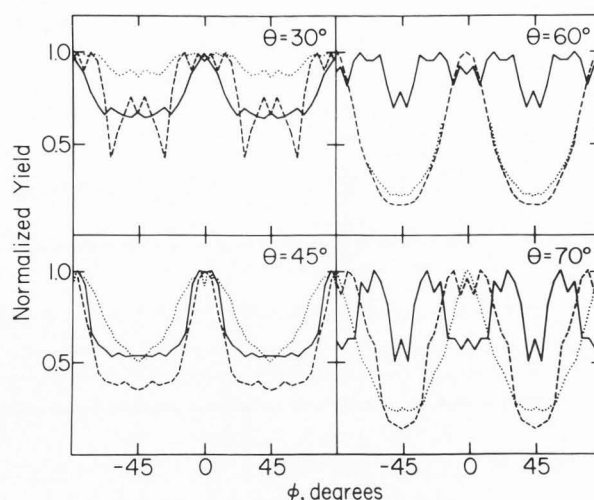


Figure 4. Predicted azimuthal dependence of the  $\text{Ni}^+$  ion yield for  $\text{Ni}(001)c(2 \times 2)\text{-CO}$  for CO adsorbed in A-top (---) and twofold sites (—). Only those particles with kinetic energies of  $3 \pm 3$  eV were counted. Experimental points (\*\*\*\*). From reference 16.

check these concepts since comparable studies have been performed on  $\text{Ni}(001)$  and  $\text{Ni}(111)$  and since a number of other experimental methods have been applied to this system. Electron energy loss spectroscopic (EELS) studies performed at 150 K suggest that the initial adsorption occurs in threefold and twofold bridge sites along the step edge. Beyond this point, the CO molecules begin to occupy terrace sites<sup>(2)</sup>. Thus, the low temperature adsorption of CO on  $\text{Ni}(7 \times 9 \times 11)$  presents a realm of interesting structural phases which should be sensitive to the azimuthal angle of incidence of the primary ion beam.

The experimental results for the  $\text{NiCO}^+$  ion yield as a function of angle is illustrated for this system in Figure 5 and the angles are defined in Figure 6. Note that the cluster ion yields are higher at  $\phi = 180^\circ$  than at  $\phi = 0^\circ$ , with the most significant variations occurring at intermediate angles. At 0.2 L exposure, the  $\text{NiCO}^+$  ion signal shows a broad peak which appears at  $\phi = 115^\circ$ . This peak shifts slightly to  $105^\circ$  and sharpens somewhat at an exposure of 0.4 L. By 0.6 L exposure the peak has become very intense and is only  $10^\circ$  wide, centered at  $\phi = 100^\circ$ . As the CO coverage increases this peak becomes very broad. At the saturation exposure of 2.8 L the  $\text{NiCO}^+$  ion intensity displays a broad maximum between  $\phi = 40^\circ$  and  $\phi = 160^\circ$ . An exposure of 0.6 L corresponds almost exactly to the exposure at which the electron energy loss spectroscopy (EELS) results indicate that all the CO molecules were bound to adsorption sites near the step edge and that all the edge sites were occupied.<sup>(2)</sup> Apparently, the specific



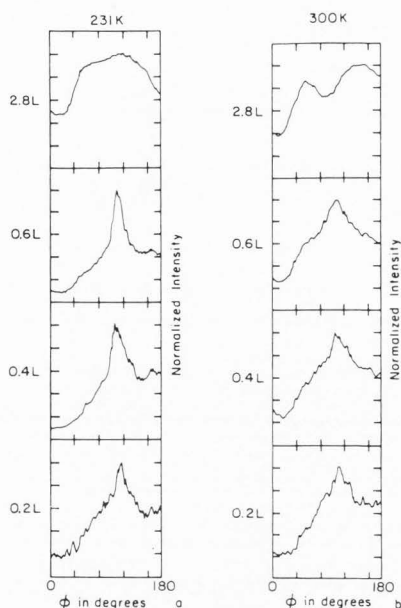


Figure 5. Normalized  $\text{NiCO}^+$  intensity versus azimuthal angle  $\phi$  as a function of CO exposure (from reference 3).

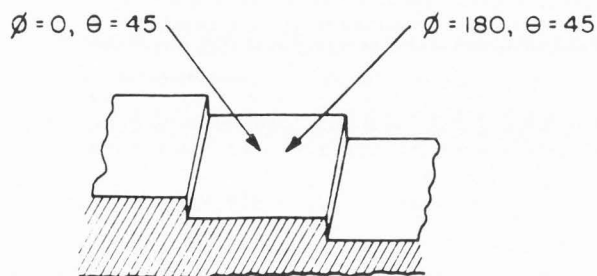


Figure 6. Definition of the polar ( $\theta$ ) and azimuthal ( $\phi$ ) angles of incidence of the primary ion beam relative to the  $\text{Ni}\{7\ 9\ 11\}$  surface (from reference 3).

bonding site of the CO next to the step edge is responsible for the sharp peak in the  $\text{NiCO}^+$  ion signal at  $\phi = 110^\circ$ . At saturation, the peak loses this definition completely, presumably since the CO molecules occupy several sites. At CO exposures performed at room temperature the azimuthal plots do not exhibit such sharp features, as illustrated in Figure 5. Calculations performed for the twofold bridge step-edge adsorption geometry corresponding to the 0.6 L exposure point successfully reproduce the sharp feature at  $\phi = 120^\circ$ , although it has not yet been possible to identify the specific collision mechanisms that cause it to occur.<sup>(3)</sup>

#### Angle-Resolved SIMS Studies of Organic Monolayers

We have seen how the angular distributions reflect the bonding geometry of adsorbates through analysis of the azimuthal anisotropies and by varying the angle of incidence of the primary ion. The next possibility is to see if there are channeling mechanisms which act perpendicularly to the surface and which manifest themselves in the polar angle distributions. The model systems which illustrate this effect are benzene and pyridine adsorbed on  $\text{Ag}(111)$  at 153 K. These model systems are of interest for a number of reasons. (i) The molecules are similar in size and shape and should behave in a closely related fashion under the influence of ion bombardment. (ii) Classical dynamics calculations have been performed on these molecules adsorbed on  $\text{Ni}(001)$  where dramatic differences in the molecule yield are predicted to occur with molecular orientation.<sup>(5)</sup> (iii) Electron energy loss spectroscopy indicates that pyridine on  $\text{Ag}(111)$  initially adsorbs in  $\pi$ -bonded configuration but undergoes a compressional phase transition to a  $\sigma$ -bonded configuration as the coverage is increased.<sup>(1)</sup> Benzene, on the other hand, is believed to remain in the  $\pi$ -bonded configuration at all coverages.<sup>(4)</sup> A more detailed discussion of these effects is presented in reference 15.

#### Angular Distributions of Neutral Atoms Desorbed from Single Crystals

Most experimental studies aimed toward determining the angular distributions of secondary particles have focussed on the measurement of the secondary ions. The reason for this emphasis is that there have been no techniques available for detecting the neutral species with monolayer sensitivity. It would be extremely valuable to be able to perform these experiments in order to obtain data that was directly comparable to the classical dynamics calculations and to get some insight into how the secondary ion fraction is affected by the take-off angle.

In this section, we describe a new apparatus and some preliminary results, aimed at providing detailed trajectory information on the ejected neutrals. It is based on a time-of-flight measurement for the neutral energies, multiphoton resonance ionization (MPRI) for the particle selectivity,<sup>(12)</sup> and two-dimensional position sensitive detection for the angular information. The detector is operated in an ultra-high vacuum environment, on well-characterized surfaces, and with low primary ion dosages onto the sample. A schematic representation of the experiment is illustrated in Figure 7. The desorption is initiated by a 0.2  $\mu\text{s}$ , 5 keV  $\text{Ar}^+$  ion pulse incident on the sample at  $45^\circ$  focussed to 0.2  $\text{cm}^2$ , and ionization is accomplished by absorption of photons from a 5 ns laser pulse obtained from the output of a Nd:YAG pumped dye laser. Under the present operating conditions we can detect neutrals whose kinetic energies vary from 0.2–50

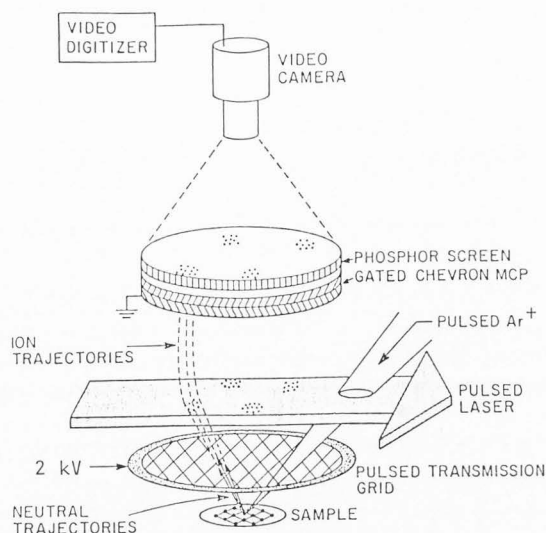


Figure 7. Detector for performing energy and angle-resolved measurement of neutrals desorbed from surfaces.

eV into a total enclosed angle of over  $100^\circ$ . A complete analysis may be performed using a total dose of less than  $10^{12}$  incident  $\text{Ar}^+$  ions/cm $^2$ . A detailed description of the apparatus will be given elsewhere.

Using this detector, we have initiated a series of experiments aimed at determining the energy and angular distributions of Rh atoms ejected from clean and adsorbate covered polycrystalline and single crystal surfaces. Rhodium atoms may be efficiently and selectively ionized using 312.4 nm laser light, obtained by frequency doubling the output of the dye laser. From the polycrystalline material, we find the velocity distribution of Rh atoms follows closely the form predicted by Thompson<sup>(14)</sup> with a peak intensity occurring at  $\sim 5$  eV and a high energy tail decreasing in intensity as  $E^{-2}$ . Polar angle distributions exhibit nearly a  $\cos^2$  shape. From a Rh{001} crystal, the velocity distribution generally peaks at a higher value than that found from the polycrystalline surface, and depends strongly on the value of the polar collection angle. For example, the energy of the emitted atoms tend to be distributed about higher kinetic energies when the polar angle is chosen to coincide with a peak in the atom intensities, a result in qualitative agreement with classical dynamics calculations.

In addition to energy distribution measurements into a given angle, we are able to extract angular distribution measurements of particles with a given energy. Polar distribution measurements at a given azimuth from Rh{001} show three peaks of preferred ejection angles. The position of these peaks are predicted well by the classical dynamics calculations as shown in Figure 8. Of particular

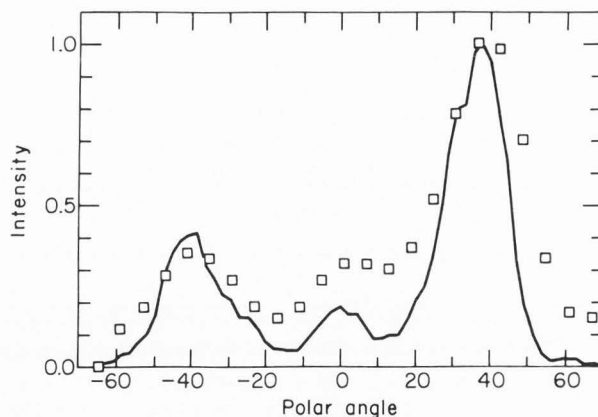


Figure 8. Measured angular distributions from clean Rh{001}. Rh atoms with kinetic energies between 2 and 34 eV are collected. The points represent experimental data while the line represents calculated results. The crystal is aligned along  $\phi = 0^\circ$ .

interest is the peak observed normal to the surface. This normal ejection peak is more prominent at 30 eV than at 10 eV which corresponds to an energy distribution with a larger high-energy tail. Variations in the relative intensity of this center peak relative to the side peaks are observed when an adsorbate such as sulfur is placed on the crystal surface. A preliminary example of this effect is shown in Figure 9. It is hoped that these variations, when coupled to computer simulations of the ion impact event, will lead to a new approach for characterizing such adsorbates.

#### Conclusions

It is hoped that the experimental examples discussed in this paper, together with the numerous comparisons to classical dynamics calculations, yield convincing evidence that the ion bombardment phenomenon is becoming well understood. Of particular interest is the fact that the trajectories of the secondary ions appear to follow reasonably closely those of the calculated neutrals. In addition, angle and energy-resolved measurements may provide a new approach to elucidation of the structure of single crystal surfaces.

#### Acknowledgements

The author is grateful for the financial support of the National Science Foundation, the Office of Naval Research and the Air Force Office of Scientific Research.

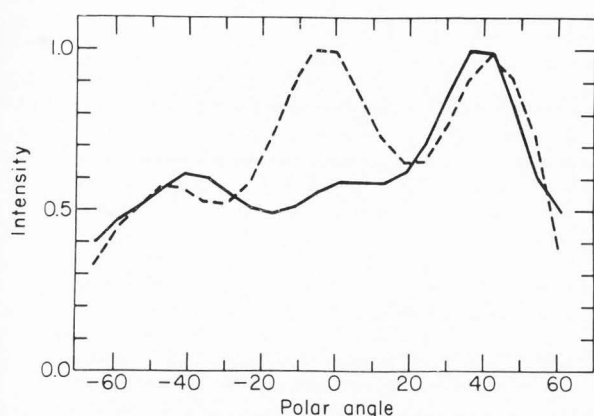


Figure 9. Measured angular distributions for clean Rh{001} (—) and Rh{001} covered with approximately 10% of a monolayer of sulfur (---). Rh between 2 and 8 eV are collected. Surface cleanliness as coverages were estimated using Auger spectroscopy.

#### References

- Demuth JE, Christmann K, and Sando PN. (1980). The Vibrations and Structure of Pyridine Chemisorbed on Ag(111): The Occurrence of a Compressional Phase Transformation. *Chem. Phys. Lett.* **76**, 201-206.
- Erley W, Ibach H, Lehwald S, Wagner H. (1979). CO Vibrations on a Stepped Ni Surface. *Surf. Sci.* **83**, 585-598.
- Foley KE, Winograd N, Garrison BJ, Harrison Jr. DE. (1984). A SIMS and Classical Dynamics Study of the Chemisorption of CO on Ni(7 9 11). *J. Chem. Phys.* **80**, 5254-5261.
- Friend F and Muetterties EL. (1981). Coordination Chemistry of Metal surfaces. 3.<sup>1</sup> Benzene and Toluene Interactions with Nickel Surfaces. *J. Am. Chem. Soc.* **103**, 773-779.
- Garrison BJ (1982). Organic Molecule Ejection from Surfaces due to Heavy Particle Bombardment. *J. Am. Chem. Soc.* **104**, 6211-6217.
- Gibbs RA, Holland SP, Foley KE, Garrison BJ, and Winograd N. (1982). Energy- and Angle-Resolved SIMS Investigation of the Ni(001)-Carbon Monoxide System. *J. Chem. Phys.* **76**, 684-695.
- Gibbs RA, Winograd N. (1981). Design and Performance of an Energy- and Angle-Resolved Secondary Ion Mass Spectrometer. *Rev. Sci. Instrum.* **52**, 1148-1155.
- Harrison Jr. DE, Moore WL, Holcombe HT, (1973). Surface Study by Application of Noble Gas Ion Backscattering Technique. *Radia. Eff.* **18**, 167-169.
- Holland SP, Garrison BJ, Winograd N. (1979). Evidence for a Recombination Mechanism of Cluster Formation from Ion Bombarded Surfaces. *Phys. Rev. Lett.* **43**, 220-223.
- Hopster H, Brundle CR. (1979). Use of SIMS for Studies of Adsorption on Well-Defined Metal Surfaces (1) Combined XPS/LEED/SIMS Studies of O<sub>2</sub>, CO, H<sub>2</sub>O, and H<sub>2</sub> on Ni(100). *J. Vac. Sci. Technol.* **16**, 548-551.
- Kapur S, Garrison BJ. (1981). Theoretical Studies of the Angular Distributions of Oxygen Atoms ejected from an Ion bombarded c(2x2) Overlayer of Oxygen on Ni(001). 1. Effect of Geometry. *J. Chem. Phys.* **75**, 445-452.
- Kimock, FM, Baxter JP, Pappas DL, Kobrin PH, Winograd N. (1984). Solid Analysis using Energetic Ion Bombardment and Multiphoton Resonance Ionization. *Anal. Chem.* **56**, 2782-2791.
- Silsbee RH. (1957). Focusing in Collision Problems in Solids. *J. Appl. Phys.* **28**, 1246-1250.
- Thompson MW. (1968). The Energy Spectrum of Ejected Atoms during the High Energy Sputtering of Gold. *Phil. Mag.* **18**, 377-414.
- Winograd N. (1981). Characterization of Solids and Surfaces using Ion Beams and Mass Spectrometry. *Progress in Solid State Chemistry* **13**, 285-375.
- Winograd N. (1984). Angle-Resolved Secondary Ion Mass Spectrometry. *Chemical Physics* **35**, Springer Series, NY, 403-426.

#### Discussion with Reviewers

**A. Lodding:** Your paper deals nearly exclusively with the angular distributions of secondary particles, and in your conclusion you state that the trajectories of secondary ions appear to follow those of the neutrals. Would you suggest that also the kinetic energy distributions of the ions and the neutrals follow more or less the same patterns? In particular, can the work you are reviewing say anything regarding the roles of mass and valency in the energy distributions of impurity ions ejected from a given matrix?



**Author:** In general, the energy distributions of secondary ions are broader and peak at higher energies than the neutrals. There are at least two reasons for this difference. First, the slow moving ions are more readily neutralized than the fast moving ones and second, the ions are more strongly attracted to the surface because of the presence of an image force. The energy distributions of impurity atoms are not believed to be mass dependent, but will be effected by how strongly they are bound into the matrix. This would indirectly be related to valency.

**R.W. Linton:** What is your view of the utility and limitations of the possible extension of the MPRI/TOF techniques to atomic and/or molecular SIMS problems requiring high lateral spatial resolution and detection sensitivity (e.g., using a pulsed liquid metal ion source)?

**Author:** These prospects are not very good since these methods are limited by the number of atoms one can transport from the solid into the laser beam. Since currents are low for focussed beams (i.e.,  $10^{-9}$  amps or lower) and the duty cycle of the experiment is only  $10^{-4}$ , only  $\sim 10^6$  atoms/sec will find themselves in the photon field. The sensitivity will, therefore, be limited to the ppm level or so. On the other hand, if the duty cycle can be increased by two orders of magnitude, the prospects do improve significantly.

**R. W. Linton:** What are typical experimental values of energy resolution, angular resolution, and detection sensitivity (secondary ion impacts/pixel-s at the detection limit) in the MPRI experiments?

**Author:** Energy resolution is about 5% for DE/E, angular resolution is  $\pm 3^\circ$  and the detector detection limit is less than 0.1 count/sec (each pixel has a background level about  $10^3$  times lower than 0.1 cps).

**J. A. Gardella:** Can you compare the results from angle resolved secondary ion and neutral distribution in terms of the image force corrections that are used for the SI distribution, and not for the secondary neutral experiment. What types of topological effects are included in the form of the image force corrections for the stepped surface case?

**Author:** As I understand the question, we have not yet been able to perform measurements of ions and neutrals on the same sample in the same apparatus. We have attempted some comparisons (see Gibbs, Holland, Foley, Garrison and Winograd, *Phys. Rev. B*, 24, 6178 (1981)) with theory, but have a long way to go before the issue is settled. The image correction unfortunately, does not include topological effects.

**J. A. Gardella:** Please comment on the effects of the compressional phase transition observed in the pyridine/Ag experiment, on the yield and origin of the secondary ions observed. How do these results impact on the two step molecular ion emission model where "desorbed" molecular and quasimolecular ions come from events at a time delayed from initial bombardment/emission of atomic and fragment ions.

**Author:** The compressional phase transition effects the yield of pyridine molecules quite dramatically. The  $\pi$ -bonded molecules receive a number of concerted low energy impacts from the substrate which provides it with some translational energy. The  $\sigma$ -bonded molecule ejects only when there is a direct collision which severs the nitrogen-metal bond. This process is of low probability and the yield of  $\sigma$ -bonded molecules is significantly reduced.